

The Magnetic Order of Cr in Fe/Cr/Fe(001) Trilayers

D. T. Pierce, J. Unguris, R. J. Celotta, and M. D. Stiles

Electron Physics Group, National Institute of Standards and Technology

Gaithersburg, MD 20899-8412

Abstract

The temperature dependence of the short period oscillatory coupling in Fe/Cr/Fe(001) whisker trilayers, when analyzed in light of recent theory, provides strong evidence that incommensurate spin density wave antiferromagnetic order is induced in the Cr over a wide range of thickness and up to temperatures at least 1.8 times the Néel temperature of bulk Cr. Because the portion of the Cr Fermi surface connected with the short period interlayer coupling in paramagnetic Cr does not exist in antiferromagnetic Cr, the conventional quantum well model of interlayer coupling is not applicable. Rather, it is necessary to use a model for the coupling that includes the electron-electron interactions that lead to the antiferromagnetic order.

Measurements of Fe/Cr multilayers have been the source of numerous important discoveries in thin film magnetism. The fundamental phenomena of exchange coupling in transition metal multilayers¹, giant magnetoresistance^{2,3}, long⁴ and short period^{5,6} oscillations in the exchange coupling with varying Cr spacer thickness, and the imaging⁷ of 90 degree biquadratic coupling were all first reported for Fe/Cr multilayers. There have been extensive studies of Fe/Cr multilayers ranging from trilayers to superlattices

with many bilayer repeats. The apparent discrepancies between results reported for different systems can be understood in a unified picture that accounts for the sensitivity of the Cr magnetic order and the interlayer exchange coupling to a variety of structural details⁸.

Directly measuring the Cr magnetic order by neutron scattering requires superlattices with both enough layers and large enough area to provide sufficient sensitivity. Depending on temperature and Cr spacer layer thickness, paramagnetic, and commensurate and incommensurate spin density wave antiferromagnetic phases are observed. With Fe whisker substrates, it is possible to grow Fe/Cr/Fe trilayers with interfaces that are much closer to ideal than those in superlattices. Unlike the superlattices, Fe/Cr/Fe trilayers are not amenable to neutron scattering measurements. The issue of whether the Cr spacer layer is paramagnetic or antiferromagnetic in the temperature and thickness ranges of interest must be inferred examining the behavior of the magnetic coupling.

The focus of this paper is to elucidate the magnetic state of Cr in optimally prepared Fe/Cr/Fe(001) whisker trilayers and the implications for the models which describe the interlayer exchange coupling. The *conventional* model for interlayer exchange coupling through a paramagnetic metal spacer layer, such as a noble metal, is the quantum well picture.^{9,10,11} The strength of the coupling depends on the reflection amplitudes of electrons at the interfaces between the paramagnetic spacer layer and the ferromagnetic layers as well as on the spacer Fermi surface geometry. The periods of the coupling are determined from the critical spanning vectors of the spacer layer Fermi surface. Thickness fluctuations of the spacer layer average the coupling, and short period

oscillations of the coupling are not observed if the thickness fluctuations are too large. An extrinsic biquadratic coupling may also be induced by thickness fluctuations.¹²

The paramagnetic Cr Fermi surface for an (001) interface is shown in Fig. 1. In Cr, there are substantial regions of the Fermi surface that are parallel, or nested, and separated by the nesting wavevector of magnitude $Q = \frac{2\pi}{a}(1 - \delta)$ where the lattice constant a is twice the layer spacing. The nesting wave vector is slightly incommensurate with the lattice wavevector $\frac{2\pi}{a}$ where δ is the incommensurability parameter. In the conventional model for interlayer exchange coupling, the nesting wavevector Q of paramagnetic Cr is the extremal spanning vector of the Fermi surface that leads to the observed short period oscillatory exchange coupling which is hence slightly incommensurate with the bcc lattice. The long period oscillatory coupling has been attributed to the extremal spanning vectors at the N-centered ellipses¹⁴.

There is also an enhancement of the magnetic susceptibility at Q that leads to a transition from paramagnetic to antiferromagnetic Cr below the Néel temperature, T_N . When Cr orders antiferromagnetically, a small gap opens at the Fermi level and that part of the nested Fermi surface connected by Q in Fig. 1 disappears¹⁵. This has been known for some time and is manifested, for example, as a resistivity anomaly at T_N in bulk Cr.¹⁵ Recent photoemission measurements that map the energy bands show explicitly that a gap opens at the Fermi level¹⁶. Because that part of the Fermi surface connected with the short period oscillations in the conventional coupling model no longer exists in antiferromagnetic Cr, it is necessary to go beyond the conventional model, which treats the spacer material in an itinerant electron picture, and include a treatment of the

electron-electron interactions of the type that stabilize the incommensurate order in Cr. Thus, the appropriate model for the short period oscillatory exchange coupling in Fe/Cr/Fe depends on whether the Cr spacer layer is paramagnetic or antiferromagnetic. In contrast, the N-centered ellipses do not differ significantly between paramagnetic and antiferromagnetic Cr and the conventional model is presumed adequate for either state.

Several descriptions of the antiferromagnetic order of Cr in Fe/Cr/Fe trilayers have been advanced. First-principle calculations show that short period oscillatory magnetic coupling occurs for both paramagnetic and antiferromagnetic Cr spacers^{18,19,20}. Recent model calculations of Shi and Fishman²¹ are particularly useful in their explanations of the temperature dependence of the Cr magnetic order. We will analyze our measurements of the temperature dependence of the coupling in light of the model calculations of Shi and Fishman²¹ and show that one is led to the conclusion that in optimally grown Fe/Cr/Fe trilayers on Fe(001) single crystal whiskers, the Cr is antiferromagnetic over a wide range of temperature and thickness.

The model calculations of Shi and Fishman²¹ consider the competition between a) the interface magnetic coupling, which maximizes the amplitude of the Cr spin density wave at the boundaries (i.e. an antinode at the Fe/Cr interface), and b) the intrinsic antiferromagnetism of the Cr spacer, which favors bulk values of the spin density wave amplitude and wave vector. The magnitude of the spin density wave ordering

wavevector $Q' = \frac{2\pi}{a}(1 - \delta')$ is always closer to commensuration than the nesting wave

vector Q , that is, $0 \leq \delta' < \delta$ ²¹. Two examples of transverse spin density waves are

shown in Fig. 2. A commensurate spin density wave, i. e., $\delta' = 0$, is shown in Fig. 2 (a).

An incommensurate spin density wave is shown in Fig. 2 (b); the nodes are separated by $1/\delta'$ ML.

We begin by reviewing the room temperature measurements^{5,22} of the interlayer coupling of trilayers where the Cr is grown as a very shallow wedge on a near perfect Fe single crystal whisker substrate as shown in Fig. 3. The oscillations in the exchange coupling with varying Cr thickness are readily observed in a Scanning Electron Microscopy with Polarization Analysis (SEMPA) image of the top Fe layer magnetization. The SEMPA image is formed by measuring the spin polarization of the secondary electrons as the SEM beam is rastered across the sample surface. Such an image is shown in Fig. 4 (b). A line scan through Fig. 4 (b) gives the measured polarization profile shown in Fig. 4 (c) of the Fe overlayer. The Fe overlayer is seen to be coupled ferromagnetically to the Fe whisker substrate for the first four layers, and then the coupling begins to oscillate. It changes from ferromagnetic coupling (white regions in Fig. 4 (b)) to antiferromagnetic (overlayer magnetization antiparallel to the whisker magnetization) and back as the Cr increases in thickness by two additional layers. The change in direction of the coupling continues with each additional Cr layer up to 24 layers. The coupling is ferromagnetic for both 24 and 25 layers of Cr and only for 26 layers does it change to antiferromagnetic. This phase slip in the coupling is repeated each 20 layers. In the conventional model of the exchange coupling, the phase slip is a beating phenomenon resulting from the slight difference between the extremal spanning vector of the Fermi surface \mathbf{Q} and the lattice wavevector.

If the Cr is antiferromagnetic^{19,20,21}, the phase slip occurs at Cr thicknesses where an additional node is introduced in the spin density wave. In this picture, the data of Fig.

4 results from changes in the Cr spacer as shown in Fig 4(a). There is commensurate spin density wave order through 24 layers. At 25 layers, a node pops in, and then there is incommensurate spin density wave order. With increasing Cr thickness, the incommensurability δ' decreases, that is the spin density wave period increases, so as to maintain maximum spin density wave amplitude at the Fe interface up through a thickness of 44 layers. At 45 layers, another node is formed in the spin density wave and the distance between nodes contracts toward bulk values. Thus, the period of the spin density wave is not rigid in these Cr films, but adjusts to match the boundary conditions. Although the internal structure of the Cr illustrated in Fig. 4 (a) cannot be measured directly for these Fe/Cr/Fe trilayers, this picture is consistent with our results. Exactly what occurs in the first few Cr layers at the interface with the Fe whisker is not known. There is evidence of interfacial alloying at the temperatures for optimal Cr growth.^{23,24} Calculations²⁵ show that 25% of the first Cr layer intermixing with the Fe is sufficient to cause the observed π phase change in the antiferromagnetic stacking of Cr. Note that the polarization profile $P(\text{Cr})$ of the Cr wedge shown in Fig. 4 (d), measured before adding the top Fe overlayer, also exhibits short period oscillations with phase slips every 20 layers²². Apparently, one Fe interface is sufficient to induce spin density wave antiferromagnetic order in the Cr.

Whereas the room temperature coupling measurements of Fig. 4 could be explained by the conventional model of interlayer exchange coupling, measurements of the position of the first phase slip at different temperatures provides definitive evidence for antiferromagnetic order in the Fe/Cr/Fe trilayers. The change in the position of the phase slip with temperature is most easily seen in measurements of the bare Cr wedge on

the Fe(001) whisker. The displacement by 14 layers of the first phase slip from its position at 24-25 layers at 310 K to 38-39 layers at 550 K is shown by the solid curved line in Fig. 5 (a). SEMPA images in the same temperature range²⁶ are also shown in Fig. 5 (a). The SEMPA images show that the long period coupling can obscure the short period coupling at higher temperatures. The magnetization direction of the short period oscillations is reversed where it can be seen above and below the phase slip line, for example at Cr thicknesses of 25 to 30 layers. The dashed line is the solid curve displaced by 20 layers to indicate where the next phase slip occurs. The temperature dependent measurements on bare Cr and on the trilayers were completely reversible.

This large temperature dependence of the position of the phase slips cannot be explained in the conventional coupling model because the temperature dependent changes in the Cr paramagnetic Fermi surface are much too small to cause a sufficient change in the nesting wavevector and hence in the incommensurability²¹. Rather, a model is required, such as that of Shi and Fishman²¹, that takes into account the electron-electron interactions in the Cr that stabilize the antiferromagnetic state. In this picture, the solid line in Fig. 5 (a) marks the transition from a commensurate spin density wave with no nodes ($n = 0$) where the Cr is thinner, to an incommensurate spin density wave with one node. The dashed line then corresponds to the $n = 1$ to 2 incommensurate to incommensurate transition. The calculated thickness and temperature dependence of these transitions is shown in Fig. 5 (b). The model gets the node-to-node distance correct assuming a 0.6% decrease in the lattice constant of Cr grown on Fe, but the phase slips occur at smaller distances than found experimentally. The overall trend of the change in the calculated phase slip position with temperature agrees well with that found

experimentally in the range of overlap. The strong temperature dependence found experimentally, and the agreement of the temperature variation calculated by Shi and Fishman, provides solid evidence that the Cr in Fe/Cr/Fe(001) trilayers is in an antiferromagnetic state. It is quite striking that incommensurate spin density wave antiferromagnetic order is induced in the Cr layers up to at least 1.8 times the bulk Néel temperature. This antiferromagnetic order that exists well above T_N of bulk Cr is due to the proximity of the Fe and the strong interfacial coupling of the Cr and Fe.

In summary, the strong temperature dependence of the thickness of the Cr film at which the phase slips occur in the short period oscillatory coupling in Fe/Cr/Fe(001) trilayers is evidence for spin density wave order in the Cr. The results are in qualitative agreement with the temperature dependence predicted by Shi and Fishman²¹ and consistent with a picture of magnetic order in the Cr consisting of a commensurate spin density wave up to the first phase slip and incommensurate spin density wave order beyond that. For the nearly ideal interfaces of these structures grown on Fe whiskers, the Fe-Cr interfacial coupling induces antiferromagnetic order in the Cr to temperatures well above the bulk Néel temperature. The short period oscillatory coupling cannot be explained in the conventional quantum well picture; instead, it is closely tied to the spin density wave order of the Cr.

Acknowledgements

We are grateful to R. S. Fishman, J. A. Stroscio, and A. Davies for helpful discussions.

This work was supported in part by the office of Naval Research.

References:

-
- ¹ P. Grünberg, R. Schreiber, Y. Pang, M.B. Brodsky and H. Sowers, Phys. Rev. Lett. **57**, 2442 (1986).
- ² M.N. Baibich, J.M. Broto, A. Fert, F. Nguyen Van Dau, F. Petroff, P. Etienne, G. Creuzet, A. Friederich, and J. Chazelas, Phys. Rev. Lett. **61**, 2472 (1988).
- ³ G. Binasch, P. Grünberg, F. Saurenbach, and W. Zinn, Phys. Rev. B **39**, 4828 (1989).
- ⁴ S.S.P. Parkin, N. More, and K.P. Roche, Phys. Rev. Lett. **64**, 2304 (1990).
- ⁵ J. Unguris, R.J. Celotta, and D.T. Pierce, Phys. Rev. Lett. **67**, 140 (1991).
- ⁶ S.T. Purcell, W. Folkerts, M. T. Johnson, N.W.E. McGee, K. Jager, J. aan de Stegge, W. B. Zeper, W. Hoving, and P. Grünberg, Phys. Rev. Lett. **67**, 903 (1991).
- ⁷ M. Rühlig, R. Schäfer, A. Hubert, R. Mosler, J. A. Wolf. S. Demokritov, and P. Grünberg, phys. stat. sol. (a) **125**, 635 (1991).
- ⁸ D. T. Pierce, J. Unguris, R. J. Celotta, and M. D. Stiles, J. Magn. Magn. Mater. **200**, 290 (1999).
- ⁹ D. M. Edwards, J. Mathon, R. B. Muniz, and M. S. Phan, Phys. Rev. Lett. **67**, 493 (1991).
- ¹⁰ M. C. Stiles, Phys. Rev. B **48**, 7238 (1993).
- ¹¹ P. Bruno, J. Magn. Magn. Mater. **121**, 248 (1993); Phys. Rev. B **52**, 411 (1995).
- ¹² J. C. Slonczewski, Phys. Rev. Lett. **67**, 3172 (1991).
- ¹³ J. C. Slonczewski, Phys. Rev. Lett. **67**, 3172 (1991).
- ¹⁴ M. D. Stiles, J. Magn. Magn. Mater. **200**, 322 (1999).
- ¹⁵ E. Fawcett, Rev. Mod. Phys. **60**, 209 (1988).
- ¹⁶ J. Schäfer, E. Rotenberg, G. Meigs, S. D. Kevan, P. Blaha, and S. Hüfner, Phys. Rev. Lett. **83**, 2069 (1999).
- ¹⁷ M. van Schilfgaarde and F. Herman, Phys. Rev. Lett. **71**, 1923 (1993).
- ¹⁸ M. van Schilfgaarde and F. Herman, Phys. Rev. Lett. **71**, 1923 (1993).
- ¹⁹ K. Hirai, Phys. Rev. B **59**, R6612 (1999).
- ²⁰ A. M. N. Niklasson, B. Johansson, and L. Nordström, Phys. Rev. Lett. **82**, 4544 (1999).
- ²¹ Z. P. Shi and R. S. Fishman, Phys. Rev. Lett. **78**, 1351 (1997); R. S. Fishman and Z. P. Shi, J. Phys.: Condens. Matter **10**, L277 (1998).
- ²² J. Unguris, R. J. Celotta, and D. T. Pierce, Phys. Rev. Lett. **69**, 1125 (1992).
- ²³ A. Davies, J. A. Stroschio, D. T. Pierce, and R. J. Celotta, Phys. Rev. Lett. **76**, 4175 (1996).
- ²⁴ B. Heinrich, J. F. Cochran, T. Monchesky, and R. Urban, Phys. Rev. **59**, 14520 (1999).
- ²⁵ M. Freyss, D. Stoeffler, and H. Dreyssé, Phys. Rev. B **56**, 6047 (1997).
- ²⁶ J. Unguris, R. J. Celotta, D. A. Tulchinsky, and D. T. Pierce, J. Magn. Magn. Mater. **198-199**, 396 (1999).

Figure Captions:

Fig. 1. A slice through the paramagnetic Cr Fermi surface for a (001) interface. The wavevector Q connects parallel "nested" regions of the Fermi surface.

Fig. 2. The solid arrows and dashed arrows represent the Cr moments on corner atom and body-center atom sites respectively. (a) Commensurate antiferromagnetic order. (b)

One period of an incommensurate spin density wave showing two nodes.

Fig. 3. A schematic view of the wedge trilayer sample structure showing the Fe(001) single crystal whisker substrate, the evaporated Cr wedge, and the Fe overlayer. The vertical scale is expanded many times.

Fig. 4. Presumed spin density wave structures at each side of the first two phase slips.^{19,20,21} (b) SEMPA image of the component of magnetization, M_x , in the Fe overlayer along the Fe whisker. The arrows mark the Cr spacer layer thicknesses where phase slips in the short period oscillations of the magnetization occur. (c) a line scan through (b) showing the measured spin polarization profile of the Fe overlayer. (d) The spin polarization of the Cr layer $P(\text{Cr})$, before depositing the Fe overlayer, after subtracting the contribution from the whisker.

Fig. 5 (a) SEMPA images of the coupling in Fe/Cr/Fe(001) at different temperatures. The phase slips measured on the bare Cr are shown by the solid gray line; the dashed line is the estimated position of the next phase slip. Note that, where visible, the short period oscillations in the SEMPA images of Fe/Cr/Fe have opposite direction above and below these lines. (b) Calculated²¹ curve showing the transition (heavy line) from commensurate order ($n=0$) to an incommensurate spin density wave with one node ($n=1$), as a function of temperature and Cr thickness. The lighter curves show the transitions between incommensurate spin density waves with different number of nodes.

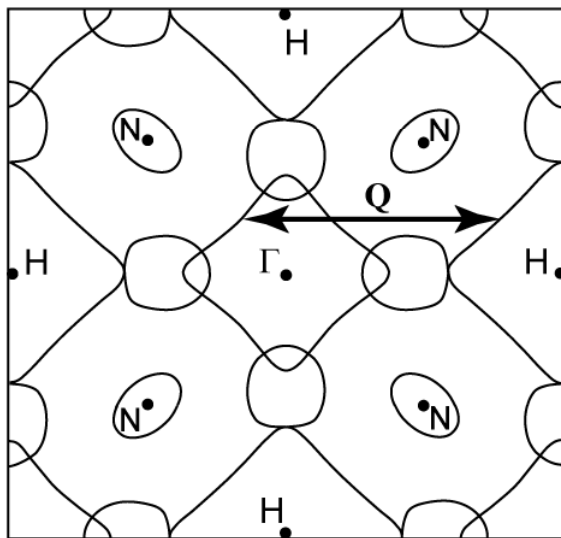


Figure 1

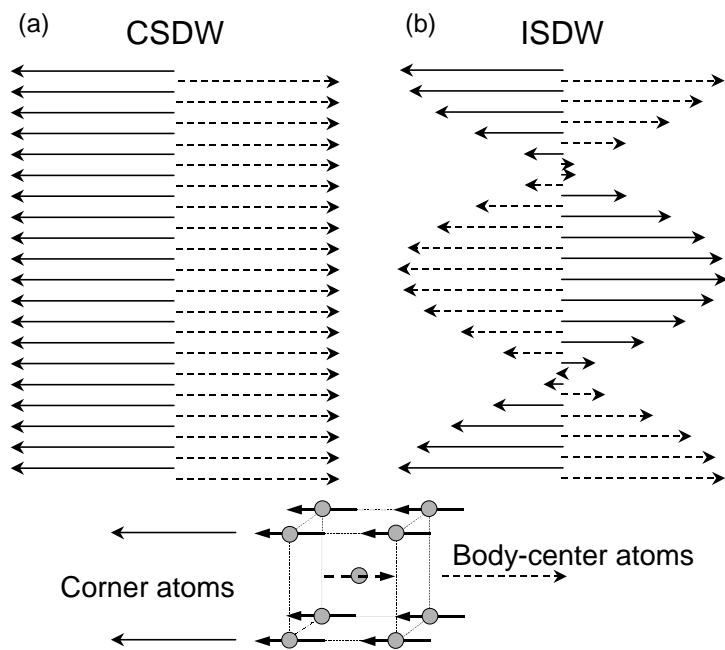


Figure 2

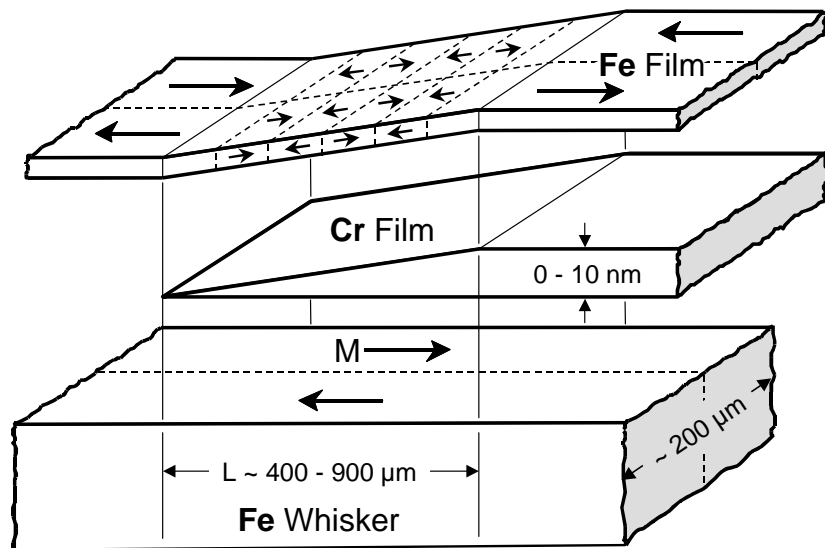


Figure 3

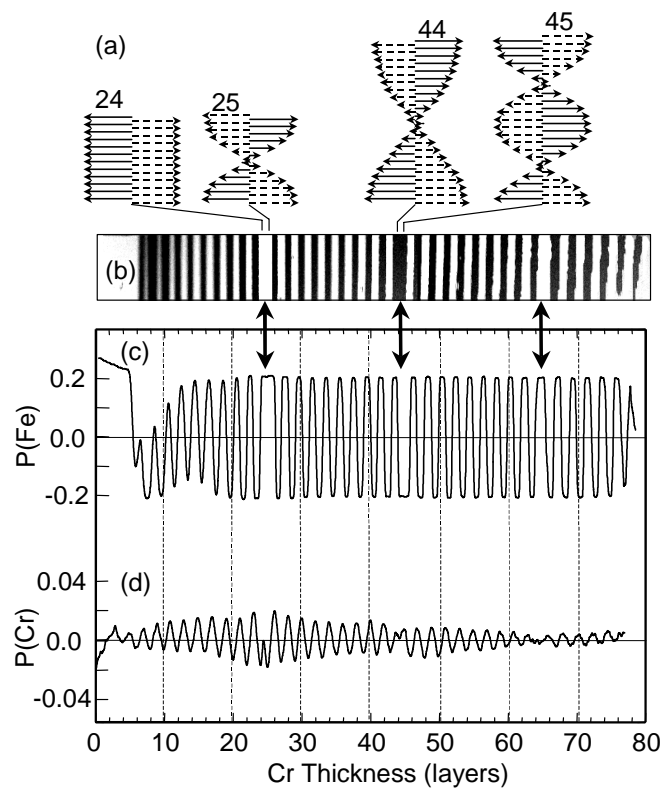


Figure 4

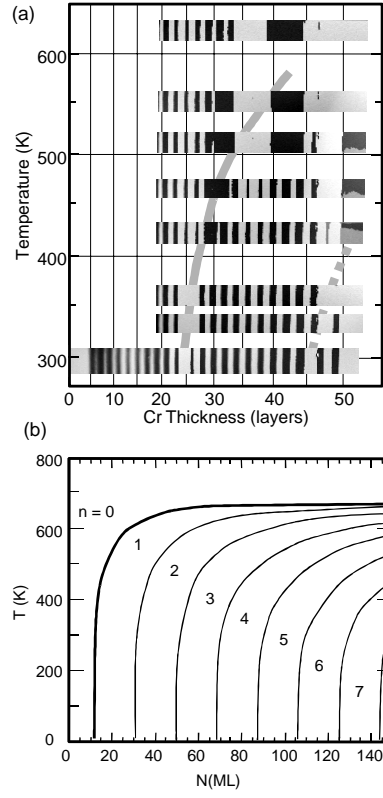


Figure 5